Biochimica et Biophysica Acta 1808 (2011) 1975–1984

Contents lists available at ScienceDirect

Biochimica et Biophysica Acta

journal homepage: www.elsevier.com/locate/bbamem

Conformational and membrane interaction studies of the antimicrobial peptide alyteserin-1c and its analogue [E4K]alyteserin-1c

Anusha P. Subasinghage [a], Donal O'Flynn [a], J. Michael Conlon [b], Chandralal M. Hewage [a,*]

[a] UCD School of Biomolecular and Biomedical Science, UCD Centre for Synthesis and Chemical Biology, UCD Conway institute, University College Dublin, Belfield, Dublin 4, Ireland
[b] Department of Biochemistry, Faculty of Medicine and Health Sciences, United Arab Emirates University, 17666 Al-Ain, United Arab Emirates

ARTICLE INFO

Article history:
Received 22 November 2010
Received in revised form 21 April 2011
Accepted 22 April 2011
Available online 30 April 2011

Keywords:
Alyteserin
Antimicrobial
AMP
NMR
Molecular modelling
Positional studies

ABSTRACT

Alyteserin-1c (GLKEIFKAGLGSLVKGIAAHVAS.NH_2), first isolated from skin secretions of the midwife toad *Alytes obstetricans*, shows selective growth-inhibitory activity against Gram-negative bacteria. The structures of alyteserin-1c and its more potent and less haemolytic analogue [E4K]alyteserin-1c were investigated in various solution and membrane mimicking environments by proton NMR spectroscopy and molecular modelling. In aqueous solution, the peptide displays a lack of secondary structure but, in a 2,2,2-trifluoroethanol (TFE-d_3)-H_2O solvent mixture, the structure is characterised by an extended alpha helix between residues Leu^2 and Val^{21}. Solution structural studies in the membrane mimicking environments, sodium dodecyl sulphate (SDS), dodecylphosphocholine (DPC), and 1,2-dihexanoyl-sn-glycero-3-phosphatidylcholine (DHPC) micelles, indicate that these peptides display an alpha helical structure between residues Lys^3 and Val^{21}. Positional studies of the peptides in SDS, DPC and DHPC media show that the N-terminal and central residues lie inside the micelle while C-terminal residues beyond Ala^{19} do not interact with the micelles.

1. Introduction

The emergence of pathogenic strains of bacteria and fungi with resistance to commonly used antibiotics constitutes a serious threat to public health and has necessitated a search for new types of antimicrobial agents [1]. Although some effective new types of antibiotics against multidrug-resistant Gram-positive bacteria, such as methicillin-resistant *Staphylococcus aureus* (MRSA) have been introduced or are in clinical trials, the situation regarding new treatment options for infections produced by emerging multidrug-resistant Gram-negative pathogens such as *Acinetobacter baumannii*, *Escherichia coli*, *Klebsiella pneumoniae*, and *Pseudomonas aeruginosa* is less encouraging [2].

Peptides with antimicrobial activity play an important role in the innate immunity that predates adaptive immunity and constitutes the first-line defence against invading pathogens for a wide range of vertebrate and invertebrate species [3]. Compounds based upon these naturally occurring anti-infective peptides are receiving serious attention as potential therapeutic agents [4]. Although there is no single mechanism by which peptides produce cell death, binding to specific receptors on the cell membrane is not involved, rather a non-specific interaction with the membrane (phospho)lipids results in disruption of membrane integrity and eventual disintegration [5].

Antimicrobial peptides are synthesized in granular glands in the skin of several, although by no means all, species of Anura (frogs and toads) and represent a source of potential therapeutically valuable anti-infective drugs [6,7]. These peptides may possess potent and broad spectrum antimicrobial activity but their therapeutic potential is often limited by their cytotoxic actions against human cells. The 23 amino acid residue peptide, alyteserin-1c was first isolated from norepinephrine-stimulated skin secretions from the midwife toad *Alytes obstetricans* and preliminary data indicated selective growth-inhibitory activity against Gram-negative bacteria but low haemolytic activity against human erythrocytes (LC_{50} = 220 μM) [8].

This study uses various NMR spectroscopic and molecular modelling methods to determine the three-dimensional solution structure of alyteserin-1c and [E4K]alyteserin-1c in various aqueous conditions and in membrane-mimetic solvent environments. Positional studies of the peptides in micellar environments were also investigated using paramagnetic probes. Our data provides insight into the structures of alyteserin-1c and [E4K]alyteserin-1c that have been useful in the development of a peptide analogue with improved therapeutic properties.

2. Materials and methods

2.1. Materials and reagents

DHPC-d_{22} micelles (1,2-dihexanoyl-*sn*-glycero-3-phosphocholine) were purchased from Avanti Polar Lipids (Alabaster, AL, USA).

Abbreviations: DHPC, 1,2-dihexanoyl-sn-glycero-3-phosphatidylcholine; DPC, dodecylphosphocholine; DSA, doxyl stearic acid; NMR, nuclear magnetic resonance; NOE, nuclear Overhauser effect; NOESY, nuclear Overhauser effect spectroscopy; SDS, sodium dodecyl sulphate; TFE, trifluroethanol; TOCSY, total correlation spectroscopy; RMSD, root mean square deviation

* Corresponding author. Tel.: +353 1 716 6870; fax: +353 1 716 6893.
E-mail address: chandralal.hewage@ucd.ie (C.M. Hewage).

0005-2736/$ – see front matter © 2011 Elsevier B.V. All rights reserved.
doi:10.1016/j.bbamem.2011.04.012

Dodecylphosphocholine (DPC), doxyl stearic acid (DSA), sodium dodecyl sulphate (SDS), CD_3OH, 2,2,2-trifluoroethanol (TFE-d_3) and 3-trimethylsilyl propionic acid (TSP) were obtained from the Sigma-Aldrich (Ireland). All other chemicals used were of analytical grade.

2.2. Synthesis of the peptide

Alyteserin-1c (GLKEIFKAGLGSLVKGIAAHVAS.NH_2) and [E4K]alyteserin-1c were supplied in crude form by GL Biochem (Shanghai) Ltd (China). The peptides were purified to near homogeneity by reversed-phase HPLC on a (2.2 cm × 25 cm) Vydac 218TP1022 (C-18) column equilibrated with acetonitrile/water/TFA (28.0/71.9/0.1, v/v/v) at a flow rate of 6 ml/min. The concentration of acetonitrile was raised to 56 % (v/v) over 60 min using a linear gradient. Absorbance was measured at 214 nm and 280 nm and the major peak in the chromatogram was collected manually. The final purity of the peptides was >98% and their identity was confirmed by electrospray mass spectrometry.

2.3. Antibacterial and haemolytic assays

Minimum inhibitory concentrations (MIC) of alyteserin-1c and [E4K]alyteserin-1c against reference strains of *E. coli* (ATCC 25922), *K. pneumoniae* (ATCC 700603), *P. aeruginosa* (ATCC 27853), *A. baumannii* (Euroclone I NM8), and *S. aureus* (ATCC 25923) were determined in duplicate in three independent experiments by a standard microdilution method using 96-well microtiter cell-culture plates [9]. In order to monitor the validity and reproducibility of the assays, incubations were carried out in parallel with increasing concentrations of antibiotics, ampicillin for *E. coli*, *A. baumannii*, and *S. aureus* and ciprofloxacin for *K. pneumoniae* and *P. aeruginosa*. Haemolytic activity against human erythrocytes taken from a healthy donor was measured as previously described [7]. The LC_{50} value was taken as the mean concentration of peptide producing 50% haemolysis in three incubations.

2.4. NMR spectroscopy

NMR experiments were performed using the 5 mm inverse probe head on Bruker DRX 500 NMR spectrometer operating at a ^1H resonance frequency of 500.13 MHz, at 298 K. 1.54 mM peptide samples were prepared in 550 µl of solvent using water, 10%, 20%, 33% and 50% TFE (d_3)-H_2O mixed solvent systems. NMR samples for micellar work were prepared by mixing 2 mg of peptide with 75 mg of 1,2-dihexanoyl-sn-glycero-3 phosphatidylcholine-d_{22} in 90:10 = H_2O:D_2O solvent mixture. This corresponds to a peptide concentration of 1.5 mM and the peptide to lipid concentration ratio of 1:200. The same protocol was used for preparing the peptide sample with 50 mg of dodecylphosphocholine and sodium dodecyl sulphate media. 2 µl of 2 mM TSP was added to the NMR sample for internal referencing. Final volume of the peptide sample was 550 µl and the pH was uncorrected.

One-dimensional (1D) proton NMR spectra and two-dimensional (2D) phase-sensitive total correlation spectroscopy (TOCSY) [10], and nuclear Overhauser effect spectroscopy (NOESY) [11] data sets were acquired with a relaxation delay of 1.5 s, acquisition time of 0.146 s, and a spectral width of 10 kHz. The TOCSY data were acquired with 40 ms and 80 ms mixing times, whereas the NOESY data were acquired with a 200 ms mixing time. The experiments were performed with 16 and 32 transients for each of 2048 t_1 increments into 8192 complex data points for the, TOCSY and NOESY data respectively. 2D data were zero-filled to 4096 data points in F_1 prior to transformation. All data sets were apodised in both dimensions using a shifted squared sinebell window function. All spectra were referenced internally to the residual ^1H signal of $F_3CCDHOD$ for TFE samples and trimethylsilylpropionic acid-d_4, sodium salt for aqueous samples, resonating at 3.98 and 0.00 ppm respectively. Data were processed using the Bruker Topspin program (version 2.1).

2.5. Mn^{2+} and spin-label experiments

The peptide samples (2 mg) were prepared separately by dissolving alyteserin-1c and [E4K]alyteserin-1c in 290 mM deuterated SDS solution in 90:10 = H_2O:D_2O solvent mixture. This corresponds to a peptide concentration of 1.54 mM and the peptide to lipid concentration ratio of 1:200 and the final volume of 550 µl. Stock solution of $MnCl_2$ was prepared in 90:10 = H_2O:D_2O solvent mixture and the NMR experiments were carried out with three concentrations of $MnCl_2$ (500 µM, 1.66 mM, and 2.30 mM). The pH of the NMR sample was adjusted to 3.50. The same protocols were followed for the NMR experiments with the peptide samples in DPC and DHPC (290 mM). For the spin-label experiments, 5-DSA and 16-DSA were dissolved in deuterated methanol. The NMR experiments were carried out by adding different concentrations of stearic acids ranging from 1.15 mM to 9.45 mM. NMR data collection was carried out 24–48 h after the sample preparation.

2.6. Structure calculations

2D NMR spectra were analysed and the spectral integration of the NOESY peaks were done using the SPARKY software version 3.110 [12]. NOESY peak volume integrals were converted into distance constraints by calibrating of nuclear Overhauser effect (nOe) intensity versus distance bonds routine of backbone, flexible side-chain and methyl proton classes with CALIBA [13]. Pseudoatoms were introduced for the protons which could not be stereospecifically assigned. Distance constraints involving fixed distances as well as those limits that could not be violated were regarded as irrelevant by the CYANA program [14]. A set of constraints was thus obtained with upper distance limits as input for further calculations. Torsional angle constraints in the −90° to −40° range were also included for $^3J_{HNH\alpha}$<6.0 Hz. Structure calculations were carried out using the CYANA program (version 3.0). Distance and torsional constraints were used as input to CYANA. Two hundred structures were randomly generated and energy minimised in CYANA, including 10,000 steps of simulated annealing, as well as 5,000 steps of conjugate-gradient minimisation. During the CYANA calculations, distance and torsional constraints were weighted using the force constants k_{NOE} = 1 kJ mol^{-1} $Å^{-2}$ and k_{Dihed_c} = 5 kJ mol^{-1} deg^{-2} respectively. Finally, the 20 structures with lowest target function values were subjected to 1,000 steps of unconstrained Powell minimisation using the Tripos force field within SYBYL (version 6.8.1) [15]. The Biopolymer module of TRIPOS software and the MOLMOL (version 2K.2) [16] graphics packages were used for final structure analysis. MOLMOL and PyMOL (version 0.99) [17] were used for structure representation. Calculated structures were analysed using the PROCHECK-NMR [18].

3. Results

3.1. Antibacterial and haemolytic activities of alyteserin-1c and [E4K] alyteserin-1c

The MIC values of synthetic alyteserin-1c and the analogue [E4K] alyteserin-1c against reference strains of bacteria and their haemolytic activities against human erythrocytes are shown in Table 1. The growth-inhibitory potency of [E4K]alyteserin-1c against reference strains of the clinically relevant Gram-negative bacteria *E. coli*, *P. aeruginosa*, *K. pneumoniae* and *A. baumannii* was between 2-fold and 4-fold greater than the naturally occurring peptide. A previous study has shown that the MIC values against clinical isolates of multidrug-resistant strains of *A. baumannii* ranged from 5–10 µM for alyteserin-1c and from 1.25 - 5 µM for [E4K]alyteserin-1c [7]. However, there was no increase in potency in the case of the Gram-positive bacterium *S. aureus*. The [E4K] alyteserin-1c analogue was significantly less haemolytic than alyteserin-1c (LC_{50}>400 µM compared with 220 µM).

Table 1
Minimum inhibitory concentrations (μM) against reference strains of bacteria and haemolytic activity (μM) against human erythrocytes of synthetic alyteserin-1c and its [E4K]alyteserin-1c analogue.

	Alyteserin-1c	[E4K]alyteserin-1c
E. coli	25	6
K. pneumoniae	50	12.5
P. aeruginosa	25	6
A. baumannii	6	3
S. aureus	250	250
LC_{50}	220	>400

3.2. Conformational analysis by NMR

3.2.1. Alyteserin-1c in an aqueous environment

One dimensional (1D) proton, two dimensional (2D) TOCSY and NOESY spectra were recorded for the alyteserin-1c in pure water. All spectra showed poor chemical shift dispersion indicating the lack of secondary structural features in water. While the NMR data acquired with 10% and 20% TFE showed no secondary structural features, NMR samples of 33% and 50% TFE showed clear chemical shift dispersion and well resolved peaks indicating secondary structure formation and folding of the peptide chain. As 50% TFE data showed no additional structural information, data obtained with 33% TFE were used for further studies. Sequence specific proton resonance assignment of alyteserin-1c in 33% TFE was achieved by the analysis of TOCSY and NOESY spectra. Almost all the spin patterns were unambiguously assigned in the TOCSY spectrum. The presence of $\alpha_iH/N_{i+1}H$ and $N_iH/N_{i+1}H$ cross peaks in the NOESY spectra led to the complete sequence specific resonance assignment of the alyteserin-1c peptide in 33% TFE. The presence of $d_{\beta N}(i,i+1)$ and $d_{NN}(i,i+1)$ connectivities of neighbouring amino acid residues supported the reliability of the resonance assignments. Clear, strong $\alpha_iH/N_{i+3}H$ medium range connectivities were observed for residues Leu^2 through to Ala^{22} except those between Ser^{12}/Lys^{15} due to signal overlapping. Most of the $\alpha_iH/N_{i+4}H$ connectivities were also identified for residues Leu^2 to Ala^{22} except for those between Lys^{15}/Ala^{19} and Ile^{17}/Val^{21}. The strong $\alpha_iH/\beta_{i+3}H$ medium range connectivities observed for residues between $Leu^2$and Val^{21} of the NOESY spectrum confirmed the α-helical nature of the peptide (Fig. 1).

3.2.2. Alyteserin-1c in SDS and DHPC micellar environments

The secondary structure of alyteserin-1c was determined in SDS micelles in order to mimic the anionic membrane environment. The peptide:SDS ratio (c/c) was set up as 1:200 and 1D proton, 2D TOCSY and NOESY spectra were collected at 307 K. Similar to the NOESY spectra obtained for the alyteserin-1c in 33% TFE, clear, strong $\alpha_iH/N_{i+3}H$ medium range connectivities were observed for residues Lys^3 through to Ser^{23} suggesting the secondary structural elements in the presence of SDS micelles. Strong $\alpha_iH/\beta_{i+3}H$ medium range connectivities were identified between residues $Lys^3$and Val^{21} except those between Phe^6/Gly^9, Ala^8/Gly^{11}, Ser^{12}/Lys^{15}, and Val^{14}/Ile^{17} due to chemical shift degeneracy. Sequence-specific resonance assignments were carried out, which led to the full and unambiguous identification of all the individual spin systems. As before, most of the $\alpha_iH/N_{i+4}H$ connectivities were also identified for residues Lys^3 to Val^{21} which are characteristic nOe patterns observe for the alpha helical peptides.

1D proton, 2D TOCSY and NOESY spectra were also recorded for alyteserin-1c in DHPC micelles in order to mimic the zwitterionic membrane environment. NMR data analysis and data interpretation showed clear characteristic medium range $\alpha_iH/N_{i+3}H$ connectivities that were identified between residues $Lys^3$and Ser^{23} except between Ser^{12}/Lys^{15}. Strong clear medium range $\alpha_iH/\beta_{i+3}H$ connectivities were identified between residues, Lys^3/Phe^6, Glu^4/Lys^7, Lys^7/Leu^{10}, Leu^{10}/Leu^{13}, Gly^{11}/Val^{14}, Ser^{12}/Lys^{15}, Gly^{16}/Ala^{19}, Ala^{18}/Val^{21} and a weak Ala^{19}/Ala^{22} cross peak confirming the presence of stable helical structure between residues $Lys^3$and Val^{21}. Some of the short and medium range connectivities could not be identified due to signal overlapping. As before, the $\alpha_iH/N_{i+4}H$ connectivities were also observed indicating characteristic alpha helical nature of the alyteserin-1c in DHPC micellar media (Fig. 2).

3.2.3. [E4K]alyteserin-1c in DPC and SDS micellar environments

NMR structural studies were carried out for [E4K]alyteserin-1c in the presence of DPC and SDS micellar media in order to modulate differences in negatively charged and zwitterionic environments. The

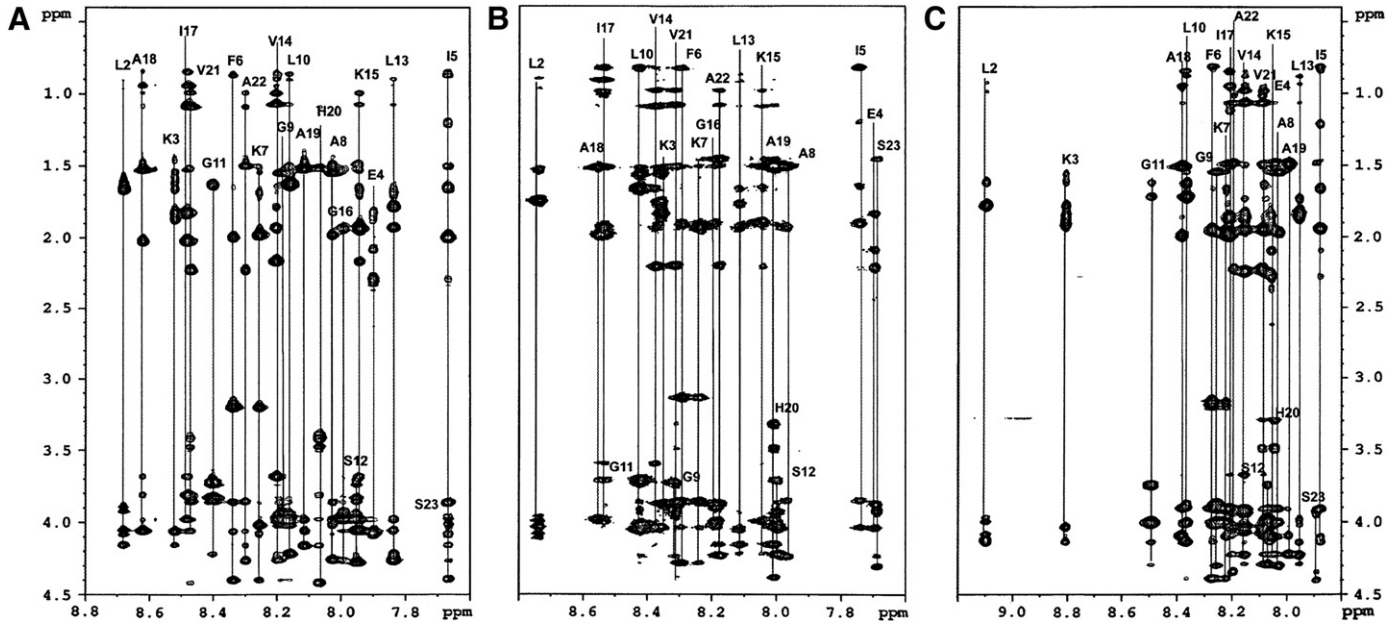

Fig. 1. NH/αH region of the NOESY spectra of alyteserin-1c in (A) 33% TFE-water; (B) SDS micelles and (C) DHPC micelles. Vertical lines represent the individual spin patterns of labelled residues.

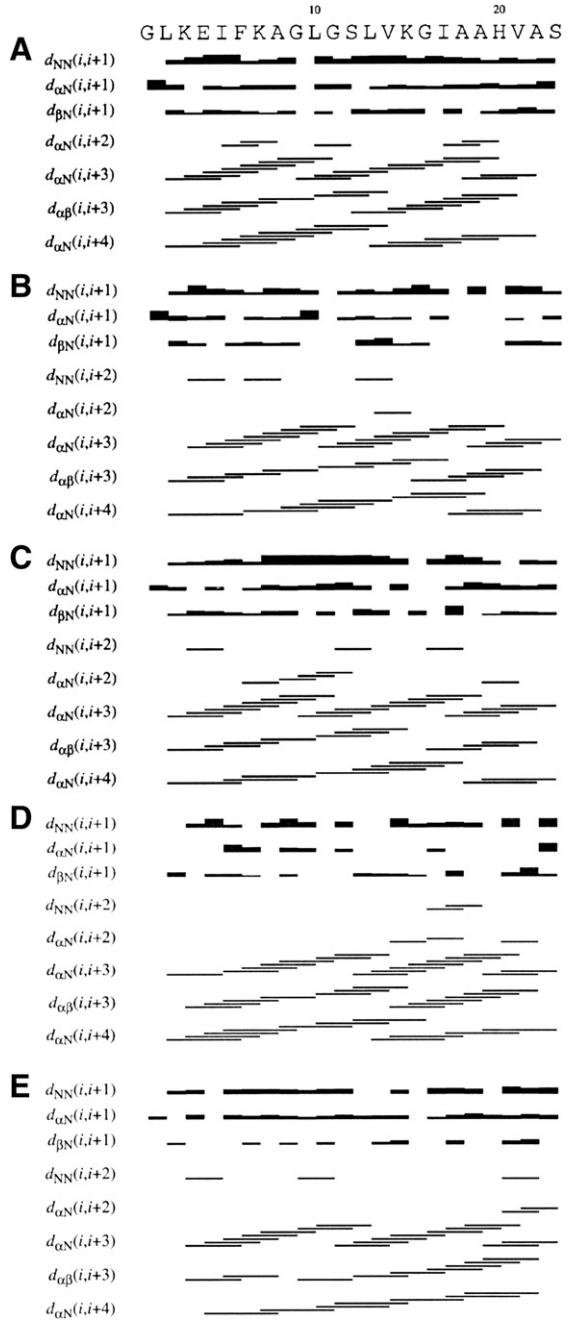

Fig. 2. Short and medium range nOe connectivities for peptide alyteserin-1c in (A) 33% TFE-water (B) SDS micelles (C) DHPC micelles and for [E4K]alyteserin-1c in (D) DPC micelles and (E) SDS micelles.

peptide:micelle ratio (c/c) was set to 1:200 as in the native peptide sample and the 1D proton, TOCSY and NOESY spectra were collected at 307 K. The NOESY spectra obtained for [E4K]alyteserin-1c in SDS were well resolved and most of the clear medium range $\alpha_iH/N_{i+3}H$ connectivities were identified in the fingerprint region except for Ala[8]/Gly[11] and Lys[15]/Ala[18] due to signal overlap. Strong medium range $\alpha_iH/\beta_{i+3}H$ connectivities were identified for those between Lys[3]/Phe[6], Ile[5]/Ala[8], Gly[9]/Ser[12], Ser[12]/Lys[15], Val[14]/Ile[17], Gly[16]/Ala[19], Ile[17]/His[20], Ala[18]/Val[21] and Ala[18]/Alal[22]. Clear, strong medium range $\alpha_iH/N_{i+4}H$ connectivities were also identified between Lys[4]/Ala[8], Lys[7]/Gly[11], Leu[10]/Val[14], Gly[11]/Lys[15], Val[14]/Ala[18], Ile[17]/Val[21] and Ala[18]/Ala[22] confirming the presence of an α-helical conformation between residues Lys[3]and Ala[22].

The nOe constraints obtained from the NOESY spectra of [E4K] alyteserin-1c in DPC media suggested that the peptide forms an alpha helical structure from Lys[3] to Ala[22]. Clear medium range $\alpha_iH/N_{i+3}H$ connectivities were identified except for Lys[3]/Phe[6] and Lys[4]/Lys[7] in the fingerprint region. Most of the strong $\alpha_iH/\beta_{i+3}H$ medium range connectivities were identified between residues Lys[3]and Ala[22] confirming the helical structural component in the presence of DPC micelles. Characteristic $\alpha_iH/N_{i+4}H$ connectivities for an α-helical peptide were also identified in the NOESY fingerprint region between Leu[2] and Ala[22].

3.3. Molecular modelling

Structure calculations for the alyteserin-1c peptide were performed based on the nOe constraints obtained for the NOESY spectra in the 33% TFE-water aqueous environment and the SDS and DHPC micellar media. For [E4K]alyteserin-1c, structure calculations were performed in DPC and SDS media. An ensemble of 200 structures was calculated randomly using the CYANA protocol and the 20 conformations that best fit the experimental constraints were subjected to additional 1000 steps of unconstrained Powell energy minimization. The calculated structure ensembles were then analysed using the PROCHECK-NMR, MOLMOL and PyMOL software packages. The main structural feature of the native peptide is a well defined right handed α-helix between residues Leu[2]and Val[21] in 33% TFE, and Lys[3] to Val[21] in the SDS and in DHPC micelles (Fig. 3). The root-mean square deviation (RMSD) values for a best fit superposition between residues 3 and 21 of backbone and heavy atoms were 0.22 ± 0.06 Å and 1.03 ± 0.19 Å for SDS and 0.49 ± 0.27 Å and 1.17 ± 0.24 Å for DHPC micellar media respectively. All ϕ/ψ values for non-glycine residues fell into allowed (73.1%), additionally allowed (26.9%) and zero generously allowed regions for DHPC in the Ramachandran plot.

The calculated structure of [E4K]alyteserin-1c indicates that the peptide forms a full length alpha helical conformation between residues

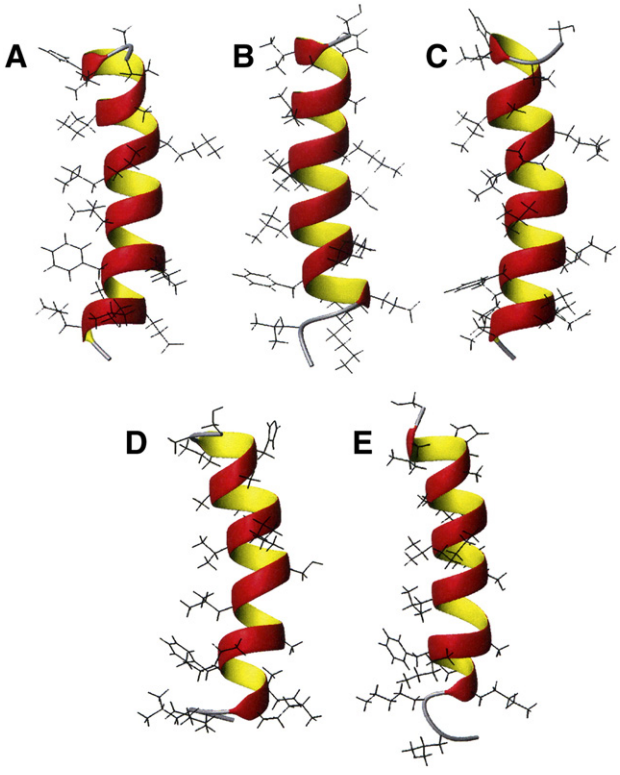

Fig. 3. Solution structure of alyteserin-1c in (A) 33% TFE-water (B) SDS micelles and (C) DHPC micelles and solution structure of [E4K]alyteserin-1c in (D) DPC micelles and (E) SDS micelles showing the ribbon representation of the average solution conformation. The N-terminus is shown at the bottom for clarity.

Lys[3] and Val[21] in both micellar environments. For [E4K]alyteserin-1c, RMSD values for a best fit superposition between residues 3 and 21 of backbone and heavy atoms were 0.39 ± 0.12 Å and 1.13 ± 0.23 Å for DPC and 0.73 ± 0.39 Å and 1.51 ± 0.34 Å for SDS micellar media respectively. All ϕ/ψ values for non-glycine residues fell into allowed (69.7%), additionally allowed (29.2%) , generously allowed (1.1%) and zero in disallowed regions for DPC in the Ramachandran plot (Table 2).

3.4. Positional studies of alyteserin-1c and [E4K]alyteserin-1c with $MnCl_2$, 5-DSA and 16-DSA

To determine the position of the alyteserin-1c in SDS and DHPC micelles, Mn^{2+} ions ($MnCl_2$), 5-DSA and 16-DSA were incorporated in to the peptide sample to induce selective broadening of resonances. For [E4K]alyteserin-1c, positional studies were carried out in DPC and SDS micellar media with Mn^{2+} and 5-DSA probes. The 1D proton and 2D TOCSY spectra with and without paramagnetic probes were recorded and compared to interpret the position of the peptide in the aqueous phase outside the membrane and within the micelle. To interpret quantitatively the results with paramagnetic broadening experiments, NH/αH cross peaks intensities of 2D TOCSY spectra were obtained using the TOPSPIN program and the remaining peak intensity/amplitude were calculated after normalizing to the least affected peak by the corresponding paramagnetic agent. These values were plotted along the sequence of the peptide (Figs. 4 and 5).

3.4.1. Mn^{2+} experiments

The peptide samples in SDS (0.5 mM) and DHPC (1.66 mM) micellar media were titrated with Mn^{2+} and the NH/αH cross peak intensity was compared with and without the paramagnetic probes. It was shown that the TOCSY cross peaks of C-terminal residues His[20], Val[21], Ala[22] and Ser[23] completely disappeared in the SDS medium while TOCSY cross peaks of Val[21], Ala[22] and Ser[23] also completely disappeared in DHPC micelles and rest of the residues showed no effects with Mn^{2+}. Similar results were also obtained for the [E4K] alyteserin-1c analogue indicating the disappearance of the TOCSY cross peaks of the C-terminal residues between His[20]and Ser[23].

3.4.2. 5-DSA and 16-DSA experiments

The 5-doxyl stearic acid (5-DSA) and 16-doxyl stearic acid (16-DSA) were incorporated into the peptide sample at different concentrations, ranging from 1.15 mM to 9.45 mM. It was shown that the 5-DSA and 16-DSA have similar effects on TOCSY cross peak intensities between residues Leu[2]and Ala[18] in both SDS and DHPC micellar media while C-terminal residues His[20] to Ser[23] showed no effects with these probes. In DHPC micelles, when 1.15 mM of either 5-DSA or 16-DSA were incorporated into the peptide sample, NH/αH cross peak intensities were slightly reduced for residues between Leu[2]and Ala[18], whereas Val[14] and Ala[18] showed a remarkable reduction in peak intensities due to peak height reduction. The NH/αH cross peak intensities for residues Glu[4], Ile[5] and Lys[15] could not be evaluated due to the signal overlapping. Upon increasing the spin label concentration of 5-DSA or 16-DSA up to 4.70 mM (Fig. 4), αH-NH cross peaks in the fingerprint region of the TOCSY spectra completely disappeared except for Ala[8], Ser[12] which showed reduced intensity and the C-terminal residues His[20] to Ser[23] showed no effect.

When 5-DSA was introduced into the SDS peptide sample, peak intensities of NH/αH TOCSY cross peaks between residues Leu[2]and Ala[18] were reduced, but there were no clear disappearances of cross peaks in the finger print region as observed with DHPC micelles. The peak intensities for Glu[4], Ile[5], Ala[8], Gly[9], Gly[11] and Ser[12] could not be obtained due to signal overlapping. At low concentration of 16-DSA, the peak intensities were slightly reduced whereas, Phe[6], Lys[7], and residues Val[14] and Lys[15] showed a remarkable reduction of peak intensity when increasing the spin label concentration up to 4.70 mM (Fig. 4). These peaks completely disappeared when increasing the 16-DSA concentration (data not shown). As before, C-terminal residues His[20] to Ser[23] showed no effect with 5-DSA and 16-DSA in SDS micelles.

TOCSY experiments were carried out for [E4K]alyteserin-1c using different concentrations of 5-DSA in SDS and DPC micellar media. It was clear that the N-terminal residues were affected by the 5-DSA up to Ala[18]. The C-terminal residues between His[20]and Ser[23] did not show any intensity changes of the TOCSY cross peaks. When 5-DSA was incorporated into the SDS micellar samples, TOCSY cross peak intensities were reduced from Leu[2] to Ala[18]. The intensities of Lys[3], Lys[7], Leu[13] and Ala[19] cross peaks could not be evaluated due to signal overlapping. For the [E4K]alyteserin-1c analogue in DPC, residues, Leu[2], Lys[3], Phe[6], Lys[7], Val[14], Ile[17] and Ala[18] were affected upon increasing the 5-DSA concentration. At high concentration of 5-DSA (9.6 mM), the TOCSY cross peaks of the N-terminal residues Leu[2] and Lys[3] completely disappeared in the fingerprint region of the TOCSY spectra while the intensities of other residues were remarkably reduced when compared to the intensities at lower concentrations of 5-DSA.

Table 2
Structural statistics of alyteserin-1c (33% TFE, DHPC and SDS) and [E4K]alyteserin-1c (DPC and SDS) micelles.

	Alyteserin-1c			[E4K]alyteserin-1c	
	33% TFE	DHPC	SDS	DPC	SDS
Total nOe constraints	237	202	221	204	205
nOe constraints used	202	176	161	156	159
nOe violations>0.2 Å	4	1	2	5	4
Ramachandran plot regions (%)					
Favoured	90.3	73.1	75.6	69.7	80.0
Additionally allowed	9.7	26.9	24.4	29.2	15.3
Generously allowed	0	0	0.7	1.1	4.7
Mean atomic RMSD (Å)					
Backbone atoms (helical)	(2–21)	(3–21)	(3–21)	(3–21)	(3–21)
	0.27 ± 0.09	0.49 ± 0.27	0.22 ± 0.06	0.39 ± 0.12	0.73 ± 0.39
Heavy atoms (helical)	0.99 ± 0.19	1.17 ± 0.24	1.03 ± 0.19	1.19 ± 0.23	1.51 ± 0.34
Average energies(kcal mol^{-1})					
Bond stretching	7.555	7.556	7.592	7.896	7.945
Angle bending	42.756	45.012	46.133	44.562	44.778
Torsional	35.925	37.823	36.84	35.340	37.227
Out of plane bending	0.303	0.378	0.327	0.428	0.294
1–4 Van der Waals	26.12	26.182	20.067	27.015	27.486
Van der Waals	-101.79	-96.936	-100.212	-95.801	-101.384
Total	10.868	20.016	16.746	19.440	16.347

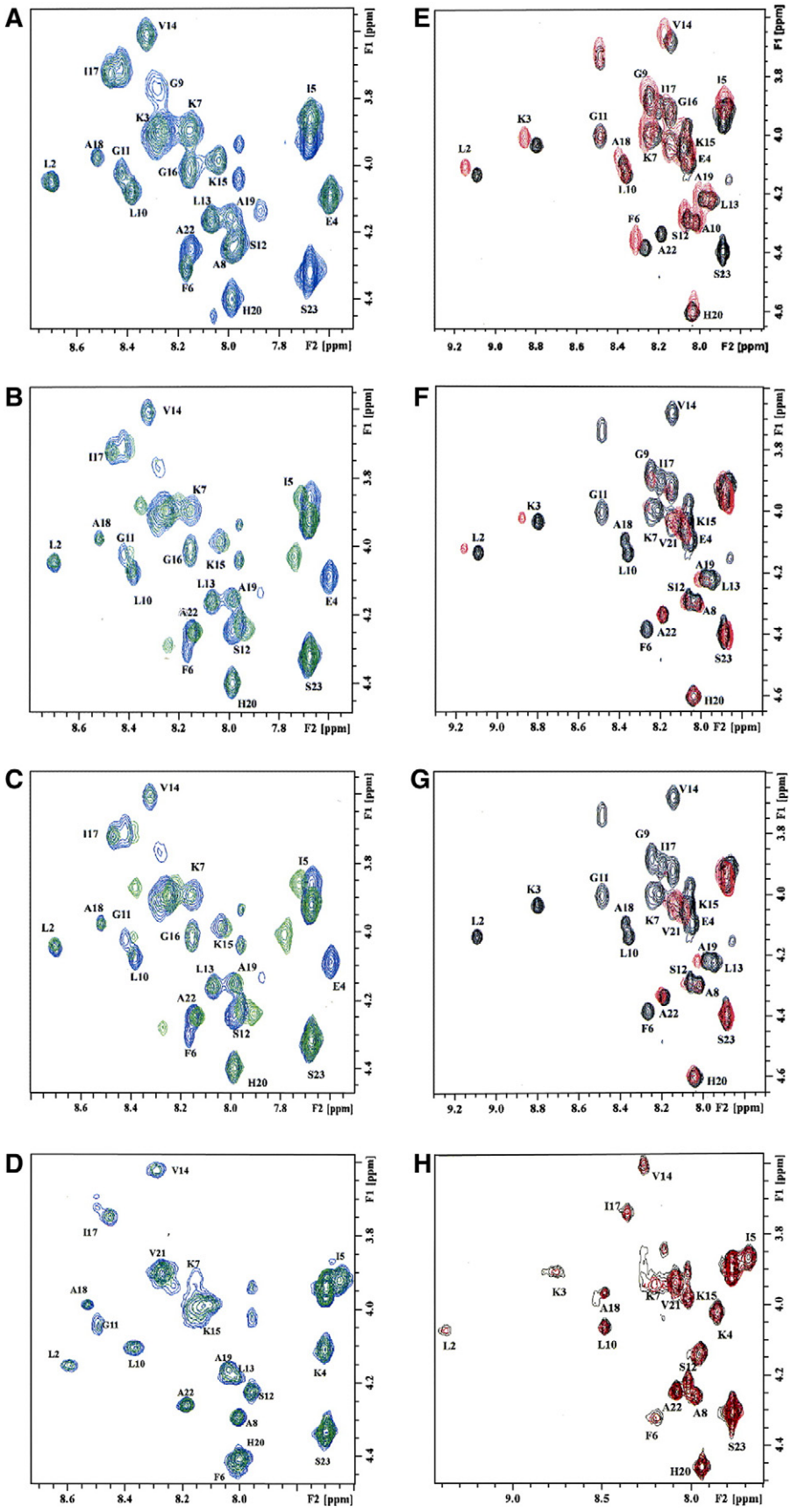

Fig. 4. 500 MHz superimposed TOCSY spectra of alyteserin-1c and [E4K]alyteserin-1c (1.54 mM) in 290 mM SDS, DPC and DHPC micellar media with and without paramagnetic agents. (4A) alyteserin-1c; 500 μM $MnCl_2$ in SDS, (4B) alyteserin-1c; 2.36 mM 16-DSA in SDS, (4 C) alyteserin-1c; 4.70 mM 16-DSA in SDS, (4D) [E4K]alyteserin-1c; 4.70 mM 5-DSA in SDS, (4E) alyteserin-1c; 1.66 mM $MnCl_2$ in DHPC, (4 F) alyteserin-1c; 2.36 mM 16-DSA in DHPC, (4 G) alyteserin-1c; 4.70 mM 16-DSA in DHPC, (4 H) [E4K]alyteserin-1c; 4.70 mM 5-DSA in DPC. All the NH/αH cross peaks were labelled with the residue number.

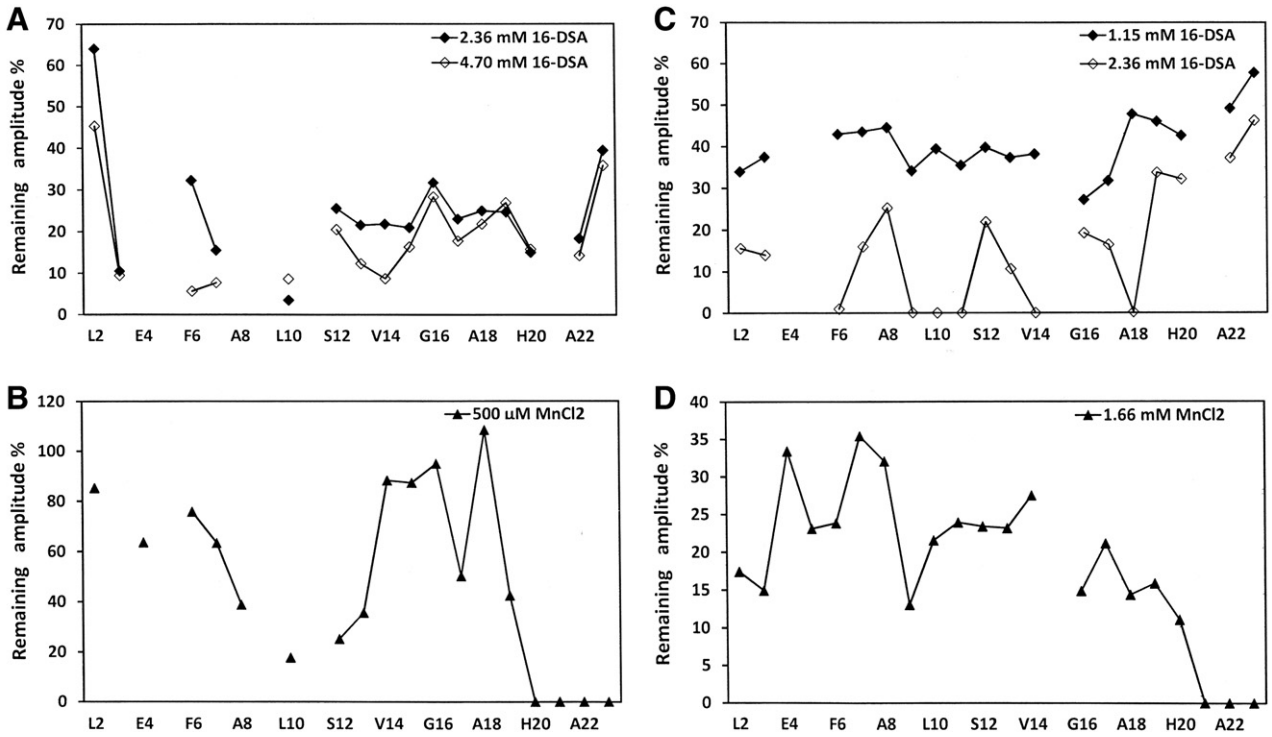

Fig. 5. Remaining amplitudes of NH/αH TOCSY cross peaks of alyteserin-1c in 290 mM SDS and DHPC micellar media after addition of paramagnetic agents. (A) Remaining amplitude when 2.36 mM and 4.70 mM 16-DSA are added to the SDS sample (B) remaining amplitude when 500 μM $MnCl_2$ is added to the SDS sample (C) remaining amplitude when 1.15 mM and 2.36 mM 16-DSA is added to the DHPC sample and (D) remaining amplitude when 1.66 mM $MnCl_2$ is added to the DHPC sample.

4. Discussion

In common with many bioactive peptides, such as peptide hormones and antimicrobial peptides, alyteserin-1c does not show any secondary structural features in aqueous medium. In 33% and 50% TFE-water mixed solvent systems, alyteserin-1c adopts an alpha helical conformation with a stable secondary structure between residues $Ile^2$and Val^{21}. It has been shown that low molecular weight fluorinated alcohols, such as TFE, may increase the amount of helical structure content of a peptide when they are added to an aqueous solution [19–22]. Fluorinated alcohols alter the electrostatic interactions within and between the peptide molecules and also tend to accumulate near the surface of the polypeptide. Consequently, they produce effects on water-solvent exposed groups, such as carbonyl and amide groups, favouring the intermolecular hydrogen bond formation which stabilizes the helical conformation [23].

In order to probe the structural basis for its specific actions against negatively charged bacterial membrane and zwitterionic mammalian membrane systems, the NMR solution structure of alyteserin-1c was investigated in SDS and DHPC micellar media, respectively. These micellar systems have served as membrane mimetic environments since the early NMR structure determination of biopolymers [24,25]. They are used as monolayers or bilayers to mimic biological membranes in NMR spectroscopic studies [26,27]. In particular, SDS micelles are used to mimic the bacterial cell membrane as it consists of a negatively charged outer surface and a hydrophobic inner core [28,29]. Similarly, DHPC micelles are used to mimic eukaryotic membrane systems that contain a higher proportion of zwitterionic phospholipids [5]. In both micellar systems, alyteserin-1c formed a well-defined amphipathic helical structure with similar backbone conformation between residues Lys^3 and Val^{21}. The side-chain orientations of the conformation vary slightly with SDS and DHPC media suggesting that alyteserin-1c may interact differently with the two micellar systems.

The three dimensional structure of the [E4K]alyteserin-1c analogue has also been determined in the presence of anionic SDS and zwitterionic DPC micelles. The calculated structure indicates that the active peptide forms a full length alpha helical conformation between residues Lys^3 and Val^{21} in both environments. The NMR and molecular modelling studies confirmed that the alyteserin-1c and the active peptide analogue, [E4K]alyteserin-1c, consist of an identical helical segment from residues Lys^3 to Val^{21}. However, side chain orientations of these peptides were different as seen in Fig. 3.

To investigate the interaction of the peptide with the various membrane environments, NMR paramagnetic experiments were performed with three different paramagnetic probes. In the aqueous phase, Mn^{2+} ions are expected to cause broadening of resonances of amino acid residues exposed to the solvent and near to the surface of micellar membrane. It is known that the doxyl stearic acids affect the inside the micellar membrane. When 5-DSA is incorporated, broadening of the resonances occurs near to the micellar boundary due to the free radical group positioned inside the micelles close to the membrane surface whereas the spin label of 16-DSA is positioned near to the centre of the micelles which will result in the reduction of peak intensity [30–32].

In SDS micelles, the C-terminal residues of alyteserin-1c are strongly affected by Mn^{2+} with cross peaks of His^{20} to Ser^{23} completely disappearing in the 2D TOCSY spectra suggesting that these residues lie outside or at the surface of the membrane. This is apparent from the remaining amplitude (Fig. 5B). Literature reports suggest that there could be a marked difference of broadening of the cross peak resonances when considering the effect of 5-DSA and 16-DSA in membrane environments [26,33]. Apart from the Gly^1 and Leu^2 residues at the beginning of the N-terminal region, most of the amino acids from Lys^3 to Ala^{18} are strongly affected by both probes. This may be explained by the fact that the micelle molecules in the solution are mobile and are continuously changing their position and shape. Due to the flexibility of micelle molecules and the hydrophobic tail of stearic acid, the effect of these two probes cannot be clearly distinguished. This resulted in a similar broadening effect for most of

the resonances in the central region of the peptide when SDS micelles were used.

In DHPC micelles, the cross peak resonances of the His^{20} residue showed reduced cross peak intensity and the cross peaks Val^{21}, Ala^{22} and Ser^{23} completely disappeared from the TOCSY spectra when $MnCl_2$ was added to the peptide samples, confirming that these residues reside outside or at the surface of the membrane. Calculated remaining amplitudes confirm that residues Val^{21} to Ser^{23} in the C-terminal region lie completely outside of the micelle (Fig. 5D). At higher concentrations of 16-DSA (2.36 mM), strong effects on the cross peak resonances were observed. In particular, cross peak resonances of Phe^{6}, Gly^{9}, Leu^{10}, and Gly^{11} completely disappeared in the TOCSY spectra while the cross peak resonances of the hydrophilic residues Lys^{3}, Lys^{7}, Ser^{12} and Lys^{15} were less affected. It is clear from the helical-wheel representation of the peptide that these residues are localized to one face of the helix (Fig. 6). It may be argued, therefore, that the peptide maintains its amphipathic nature when interacting with a membrane environment.

When the 16-DSA concentration is increased to 4.70 mM, cross peak resonances from residues Leu^{2} to Lys^{7} completely disappeared but not those of Ala^{8} and Ser^{12} (Figs. 4F, G and 5C). According to these paramagnetic broadening studies, it is clear that alyteserin-1c is located inside the micelles up to residue Ala^{18} with the hydrophobic residues facing the interior of the micelle and the hydrophilic residues facing the exterior of the membrane. All the studies indicate that the C-terminal domain from His^{20} to Ser^{23} is located outside the membrane residing in the solvent environment. Fig. 7 shows how alyteserin-1c could interact with the micellar environment.

With Mn^{2+} probe studies, the more potent analogue, [E4K] alyteserin-1c showed similar results as the parent peptide, alyteserin-1c in both SDS and DPC micellar environments showing that the C-terminal residues His^{20} to Ser^{23} lie outside of the micelle. The paramagnetic probe studies of [E4K]alyteserin-1c with 5-DSA showed a general reduction in cross peak intensity between residues $Leu^{2}$and Ala^{18} while the peak intensities for Glu^{4}, Ala^{8}, Ser^{12} and Gly^{16} were not affected to the same degree for those signals that are not overlapping. For alyteserin-1c in DHPC, the oscillating behaviour of the remaining amplitude, which is most pronounced in the 2.36 mM concentration of 16-DSA, increases for residues Ala^{8}, Ser^{12} and Gly^{16} and decreases in between these residues (Fig. 5). A similar but less pronounced pattern can be seen for alyteserin-1c in SDS. However, due to signal overlap only residues Glu^{4}, Ser^{12} and Gly^{16} could be examined (Fig. 5A). For [E4K]alyteserin-1c a similar trend can also be seen when the TOCSY cross peaks intensities for residues Lys^{4}, Ala^{8}, Ser^{12} are examined (data not shown). These results indicate that residues Glu^{4}/Lys^{4}, Ala^{8}, Ser^{12} and Gly^{16} could be closer to the hydrophilic face of the amphiphathic alpha helix suggesting that the peptides lie with the hydrophilic side facing outwards the micelle head groups (Fig. 6). However it is not possible to determine how deeply the peptide is inserted into the micelle due to the flexible nature of the DSA and the micelle molecules [26].

The micellar systems that have been used for these studies are frequently used for paramagnetic experiments to probe the conformations of antimicrobial peptides. In particular SDS is used to mimic anionic prokaryotic membrane systems whereas DHPC and DPC are normally used as a zwitterionic membrane model. Literature reports suggest that these micelle systems form a spherical shape with a diameter of 40–50 Å [29,33–35]. However, the DHPC micelle may be more accurately modelled as a barrel with the molecules arranged cylindrically around it [35]. It has also been reported that these micelle systems can change their shape in free solution due to the flexibility of the micelle molecules [26]. According to our paramagnetic experiments, it was clear that both alyteserin-1c and [E4K] alyteserin-1c peptides inserted in to the micelle membrane up to

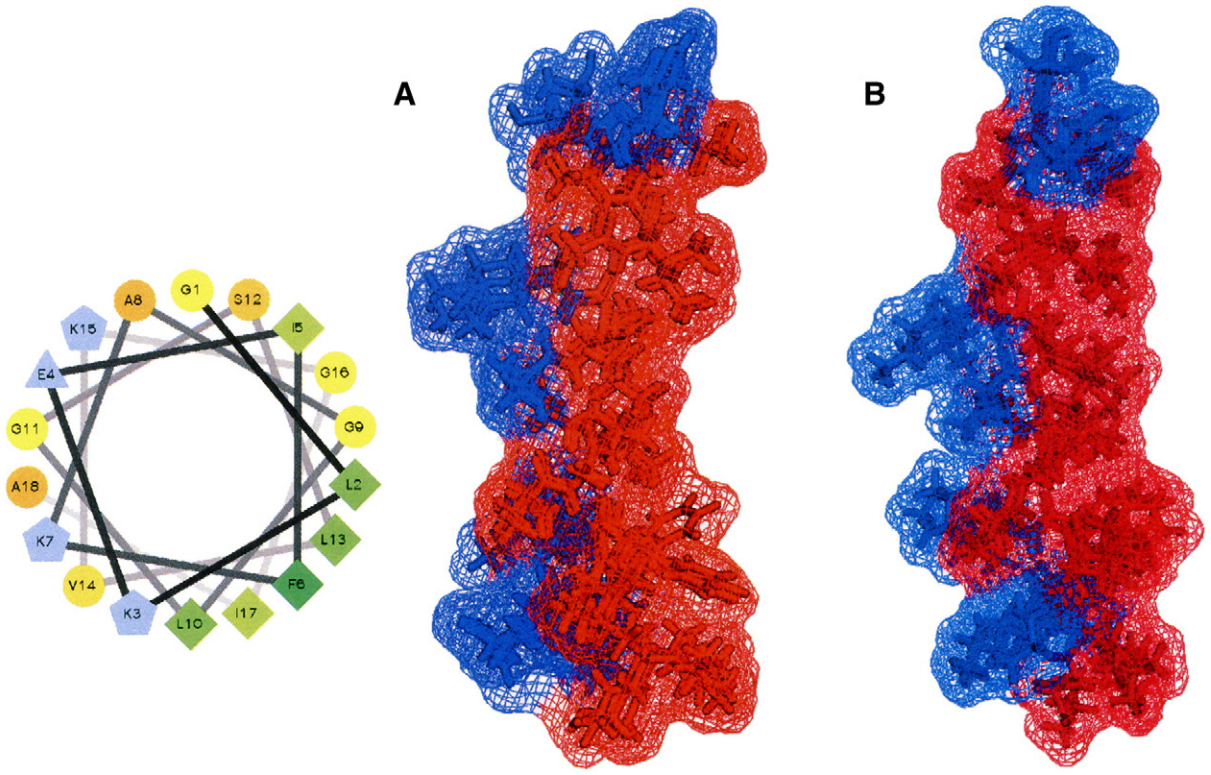

Fig. 6. Helical wheel representation and the solution structure of alyteserin-1c (6A) in DHPC micellar medium and [E4K]alyteserin-1c (6B) in SDS micellar medium demonstrating the amphipathic character and side chain orientation. The figures depict the hydrophobic (red) and hydrophilic (blue) domains of the peptides showing the N-terminus at the bottom.

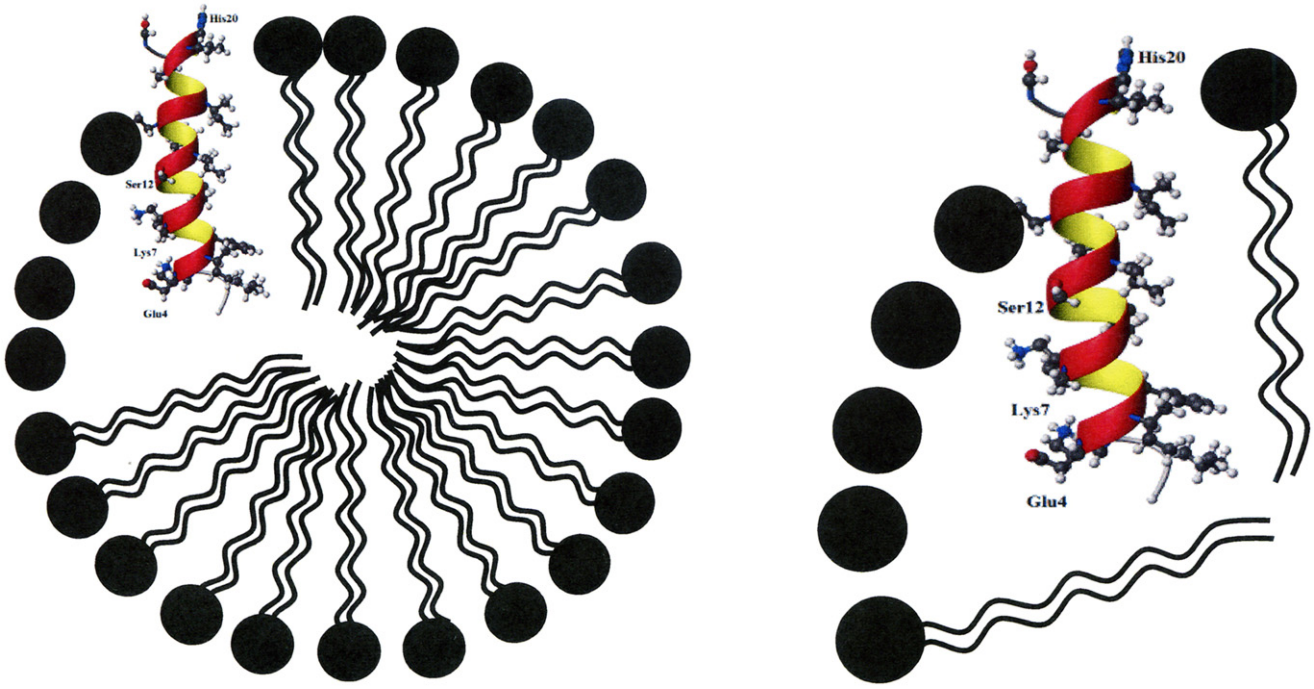

Fig. 7. Schematic representation of alyteserin-1c in a micellar environment consistent with the results obtained with paramagnetic agents. The NMR derived solution conformation of alyteserin-1c is shown with a ribbon representation and labelled hydrophilic residues. Residue 19 is at the surface of the micelle while C-terminal residues 20–23 lie outside of the micelle.

residue Ala^{18} which is approximately 4–5 helical turns. Therefore, the size of the micelle should be large enough to accommodate the peptide inside the micelle.

It is concluded, therefore, that in both micellar systems, Mn^{2+} ions have effects on the C-terminal residues from His^{20} to Ser^{23} confirming that the C-terminal region is exposed to the aqueous medium and is not interacting with the membrane. Studies of alyteserin-1c with 5-DSA and 16-DSA showed similar TOCSY cross peak intensity changes confirming that the N-terminal and central residues between Leu^{2}and Ala^{18} lie inside the micelle. Similar results were also observed for the paramagnetic probe studies of [E4K]alyteserin-1c showing that residues Leu^2 to Ala^{18} reside inside the micelle environment. These results confirm that the different segments of the alyteserin-1c and [E4K]alyteserin-1c molecules interact similarly with the micelle environments and the peptides are inserted into the membrane with the C-terminal end not interacting with the micelles. However, in terms of secondary structure, NMR structural studies of these peptides in micellar environments did not show any clear indication of why an increase in biological activity of the analogue peptide was observed. Probably, experiments in the presence of lipids instead of micelles would have been more appropriate to do the structural studies of these peptides and to get a structural interpretation of the differences in biological activity of these peptides.

Carbapenems are among the few useful antibiotics against multi-drug resistant Gram-negative bacteria so that the emergence of Enterobacteriaceae strains producing metallo-beta lactamases, such as the NDM-1 enzyme, capable of hydrolysing carbapenems and structurally related agents seriously limits treatment options [36]. A previous study has shown that the frog skin peptide ascaphin-8 potently (MIC$\leq$25 μM) inhibits growth of strains of extended spectrum beta-lactamase (ESBL)-producing *E. coli* and *K. pneumoniae* [37]. This present study identifies alyteserin-1c as a second candidate for development into an agent for treatment of infections produced by beta lactamase-producing Gram-negative bacteria. The demonstration that residues Leu^2 to Lys^7 of the peptide are of particular importance in interaction with the bacterial cell membrane has facilitated the design of an analogue ([E4K]alyteserin-1c) with increased antimicrobial potency against reference strains of these pathogens and against *P. aeruginosa* and *A. baumannii* (Table 1).

The antimicrobial potency of a peptide against microorganisms and its cytotoxicity against mammalian cells, such as erythrocytes, is determined by complex interactions among cationicity, hydrophobicity, α-helicity and amphipathicity [5]. Studies with a range of naturally occurring and model peptides (reviewed in [38]) have shown that an increase in peptide cationicity promotes interaction with the negatively charged (phospho)lipids in the bacterial cell membrane and so increases antimicrobial potency. In contrast, the plasma membrane of eukaryotic cells, such as erythrocytes, contains a higher proportion of zwitterionic phospholipids and similar studies with a range of antimicrobial peptides have indicated that increasing overall hydrophobicity increases cytotoxicity against mammalian cells. Consequently, the increase in peptide cationicity associated with the substitution Glu^4→Lys in the critically important Leu^2 to Lys^7 region of the peptide promotes stronger interaction with the negatively charged bacterial cell membrane and so results in increased antibacterial activity. The haemolytic activity of the [E4K] alyteserin-1c analogue is significantly lower than the naturally occurring peptide (LC_{50}>400 μM vs 220 μM) which may be a consequence of the small decrease in hydrophobicity associated with a lysine side-chain compared with a glutamic acid side-chain [39].

Acknowledgments

We are grateful to University College Dublin for Research Demonstrator ship to AS and DOF. Authors would like to acknowledge the funding from Science Foundation Ireland to AS and for the NMR spectrometer upgrade, and to the United Arab Emirates University for a Faculty Support Grant (NP-10-11/103) to JMC. Authors would like to thank Prof. Lena Maler, Department of Biochemistry and Biophysics, Stockholm University, Sweden for valuable input regarding the membrane interaction studies with paramagnetic agents. Structural coordinates and chemical shifts for alyteserin-1c were deposited in the PDB (2L5R) at BMRB (17281).

References

[1] S.R. Norrby, C.E. Nord, R. Finch, Lack of development of new antimicrobial drugs: a potential serious threat to public health, Lancet Infect Dis 5 (2005) 115–119.
[2] D.M. Livermore, Has the era of untreatable infections arrived? J Antimicrob Chemother 64 (2009) i29–i36.
[3] G. Diamond, N. Beckloff, A. Weinberg, K.O. Kisich, The roles of antimicrobial peptides in innate host defense, Curr Pharm Des 15 (2009) 2377–2392.
[4] J.M. Conlon, The therapeutic potential of antimicrobial peptides from frog skin, Revs Med Microbiol 15 (2004) 17–25.
[5] M.R. Yeaman, N.Y. Yount, Mechanisms of antimicrobial peptide action and resistance, Pharmacol Rev 55 (2003) 27–55.
[6] A.C. Rinaldi, Antimicrobial peptides from amphibian skin: an expanding scenario, Curr Opin Chem Biol 6 (2002) 799–804.
[7] J.M. Conlon, E. Ahmed, T. Pal, A. Sonnevend, Potent and rapid bactericidal action of alyteserin-1c and its [E4K] analog against multidrug-resistant strains of *Acinetobacter baumannii*, Peptides 31 (2010) 1806–1810.
[8] J.M. Conlon, A. Demandt, P.F. Nielsen, J. Leprince, H. Vaudry, D.C. Woodhams, The alyteserins: two families of antimicrobial peptides from the skin secretions of the midwife toad *Alytes obstetricans* (Alytidae), Peptides 30 (2009) 1069–1073.
[9] Methods for Dilution Antimicrobial Susceptibility Tests for Bacteria that Grow Aerobically, Approved Standard M07-A8, Clinical Laboratory and Standards Institute CLSI, Wayne, PA, 2008.
[10] A. Bax, D.G. Davis, MLEV-17 based two-dimentional homonuclear magnetisation transfer spectroscopy, J Magon Reson 65 (1985) 355–360.
[11] A. Kumar, R.R. Ernst, K. Wuthrich, A two-dimensional nuclear Overhauser enhancement (2D NOE) experiment for the elucidation of complete proton–proton cross-relaxation networks in biological macromolecules, Biochem Biophys Res Commun 95 (1980) 1–6.
[12] T.D. Goddard, D.G. Kneller, Sparky 3 software, University of California, San Francisco, USA, 2006.
[13] P. Guntert, W. Braun, K. Wuthrich, Efficient computation of three-dimensional protein structures in solution from nuclear magnetic resonance data using the program DIANA and the supporting programs CALIBA, HABAS and GLOMSA, J Mol Biol 217 (1991) 517–530.
[14] P. Guntert, C. Mumenthaler, K. Wuthrich, Torsion angle dynamics for NMR structure calculation with the new program DYANA, J Mol Biol 273 (1997) 283–298.
[15] Tripos Inc, South Janley Road, St. Louis, MO 63144–2319, USA, 1699.
[16] R. Koradi, M. Billeter, K. Wuthrich, MOLMOL: a program for display and analysis of macromolecular structures, J. Mol. Graph. 14 (1996) 51–55, 29–32.
[17] W.L. DeLano, The PyMOL Molecular Graphics System, DeLano Scientific, San Carlos, CA, 2002.
[18] R.A. Laskowski, J.A. Rullmannn, M.W. MacArthur, R. Kaptein, J.M. Thornton, AQUA and PROCHECK-NMR: programs for checking the quality of protein structures solved by NMR, J Biomol NMR 8 (1996) 477–486.
[19] F.D. Sonnichsen, J.E. Van Eyk, R.S. Hodges, B.D. Sykes, Effect of trifluoroethanol on protein secondary structure: an NMR and CD study using a synthetic actin peptide, Biochemistry 31 (1992) 8790–8798.
[20] A.P. Subasinghage, J.M. Conlon, C.M. Hewage, Development of potent anti-infective agents from *Silurana tropicalis*: conformational analysis of the amphipathic, alpha-helical antimicrobial peptide XT-7 and its non-haemolytic analogue [G4K]XT-7, Biochim Biophys Acta 1804 (2010) 1020–1028.
[21] I. Alana, J.P. Malthouse, F.P. O'Harte, C.M. Hewage, The bioactive conformation of glucose-dependent insulinotropic polypeptide by NMR and CD spectroscopy, Proteins 68 (2007) 92–99.
[22] C. Landon, H. Meudal, N. Boulanger, P. Bulet, F. Vovelle, Solution structures of stomoxyn and spinigerin, two insect antimicrobial peptides with an alpha-helical conformation, Biopolymers 81 (2006) 92–103.
[23] R.C. Neuman Jr., J.T. Gerig, Interactions of 2,2,2-trifluoroethanol with melittin, Magn Reson Chem 47 (2009) 925–931.
[24] L.R. Brown, K. Wuthrich, NMR and ESR studies of the interactions of cytochrome c with mixed cardiolipin-phosphatidylcholine vesicles, Biochim Biophys Acta 468 (1977) 389–410.
[25] K. Wuthrich, C. Bosch, L.R. Brown, Conformational studies of lipid-bound polypeptides by elucidation of proton–proton cross-relaxation networks, Biochem Biophys Res Commun 95 (1980) 1504–1509.
[26] P. Damberg, J. Jarvet, A. Graslund, Micellar systems as solvents in peptide and protein structure determination, Methods Enzymol 339 (2001) 271–285.
[27] G.D. Henry, B.D. Sykes, Methods to study membrane protein structure in solution, Methods Enzymol 239 (1994) 515–535.
[28] E.F. Haney, H.N. Hunter, K. Matsuzaki, H.J. Vogel, Solution NMR studies of amphibian antimicrobial peptides: linking structure to function? Biochim Biophys Acta 1788 (2009) 1639–1655.
[29] M. Lindberg, A. Graslund, The position of the cell penetrating peptide penetratin in SDS micelles determined by NMR, FEBS Lett 497 (2001) 39–44.
[30] E. Barany-Wallje, A. Andersson, A. Graslund, L. Maler, NMR solution structure and position of transportan in neutral phospholipid bicelles, FEBS Lett 567 (2004) 265–269.
[31] J. Jarvet, J. Zdunek, P. Damberg, A. Graslund, Three-dimensional structure and position of porcine motilin in sodium dodecyl sulfate micelles determined by 1H NMR, Biochemistry 36 (1997) 8153–8163.
[32] M. Lindberg, H. Biverstahl, A. Graslund, L. Maler, Structure and positioning comparison of two variants of penetratin in two different membrane mimicking systems by NMR, Eur J Biochem 270 (2003) 3055–3063.
[33] M. Lindberg, J. Jarvet, U. Langel, A. Graslund, Secondary structure and position of the cell-penetrating peptide transportan in SDS micelles as determined by NMR, Biochemistry 40 (2001) 3141–3149.
[34] M. Franzmann, D. Otzen, R. Wimmer, Quantitative use of paramagnetic relaxation enhancements for determining orientations and insertion depths of peptides in micelles, Chembiochem 10 (2009) 2339–2347.
[35] E. Papadopoulos, K. Oglecka, L. Maler, J. Jarvet, P.E. Wright, H.J. Dyson, A. Graslund, NMR solution structure of the peptide fragment 1–30, derived from unprocessed mouse Doppel protein, in DHPC micelles, Biochemistry 45 (2006) 159–166.
[36] K. Bush, Alarming beta-lactamase-mediated resistance in multidrug-resistant Enterobacteriaceae, Curr Opin Microbiol 13 (2010) 558–564.
[37] A. Eley, M. Ibrahim, S.E. Kurdi, J.M. Conlon, Activities of the frog skin peptide, ascaphin-8 and its lysine-substituted analogs against clinical isolates of extended-spectrum beta-lactamase (ESBL) producing bacteria, Peptides 29 (2008) 25–30.
[38] J.M. Conlon, N. Al-Ghaferi, B. Abraham, J. Leprince, Strategies for transformation of naturally-occurring amphibian antimicrobial peptides into therapeutically valuable anti-infective agents, Methods 42 (2007) 349–357.
[39] D.M. Engelman, T.A. Steitz, A. Goldman, Identifying nonpolar transbilayer helices in amino acid sequences of membrane proteins, Annu Rev Biophys Biophys Chem 15 (1986) 321–353.